

Contents lists available at ScienceDirect

Composites Part B

journal homepage: http://ees.elsevier.com



Vulnerability assessment of Structural Insulated Panels with metal skins subjected to windborne debris impact

Dikshant Saini a,*, Behrouz Shafei b

- a Graduate Research Assistant, Department of Civil, Construction, and Environmental Engineering, Iowa State University, Ames, IA, 50011, USA
- b Assistant Professor, Department of Civil, Construction, and Environmental Engineering, Department of Materials Science and Engineering, Iowa State University, Ames, IA, 50011, USA

ARTICLE INFO

Keywords Perforation resistance Composite panels Impact simulations Windborne debris hazard

ABSTRACT

Structural Insulated Panels (SIPs), which consist of a composite of an insulating polymer foam sandwiched between two layers of structural skins, are widely used in residential and commercial buildings. Such panels, in the regions prone to hurricanes and tornadoes, are often exposed to the risk of windborne debris impact. Despite the consequences associated with damage to SIPs, the studies on their perforation resistance and design variables have been rather limited. To address this gap, the current study develops a computational framework to assess the vulnerability of the SIPs of various configurations subjected to a range of windborne debris impact scenarios. For this purpose, impact simulations are conducted to quantify the response and evaluate the extent of damage to the SIPs. The study is further extended to evaluate the effect of various structural details and material properties on the perforation resistance of the SIPs. Based on the simulation results, a set of vulnerability curves are developed for the first time to capture the risk of failure of the SIPs under the windborne debris hazard. This is expected to improve the design of this important category of wall panels, especially to ensure their safety and performance during severe windstorms.

1. Introduction

Windborne debris impact is one of the main sources of damage to building envelopes during strong wind events, such as hurricanes and tornados. In particular, if the impact leads to a perforation, an immediate risk to the safety of occupants is anticipated. The consequences can be further expanded, as an impact-induced opening changes the internal pressure of the building, triggering extensive damage to structural and nonstructural building components. Among the most common building envelopes, Structural Insulated Panels (SIPs) are categorized as high-performance composite panels used in several residential and commercial buildings. The SIPs commonly consist of an expanded polystyrene (EPS) foam sandwiched between two structural skins of materials, such as galvalume/zincalume steel, stainless steel, fiberglass, and oriented strand board (OSB). The thickness of the SIPs can vary from 50 mm (2 in.) to 300 mm (12 in.), depending on their applications. The EPS foam is lightweight and has a closed-cell insulation structure, which features low water absorption and vapor permanence, further to high energy saving advantages [1,2]. Owing to the superior strength of the SIPs, they are deemed an appropriate composite panel system to resist impact-induced forces. This, however, has remained largely unexplored, as there are currently no guides/details for the optimal design of the SIPs in the regions prone to windborne debris hazard.

Although a number of different wall panels have been developed and tested to date, there has been growing interest in transitioning from conventional wall panels to SIPs, mainly because of the insula-

From a holistic review of the existing literature, there are a number of studies on the effect of windborne debris impact on various wall panels [3-9]. Among them, Scheer [8] conducted large missile tests on different wall and roof assemblies. The performed tests documented the extent of damage that such assemblies can experience under debris hazard. Frye et al. [3] investigated the response of metal cladding wall systems subjected to windborne debris impact loads. It was observed that an increase in the flexibility of the wall can enhance the energy absorption capacity and provide an improved resistance against impact loads. Peters and Robertson [9] tested multiple safe room's wall panels that consisted of either wood studs or cold form steel studs. The study reported how such panels can be vulnerable to the risk of windborne debris impact. In a separate effort, Zhou et al. [4] proposed a design for tornado safe rooms using carbon fiber-reinforced hybrid matrix composite (CHMC). The study also demonstrated how the wood studded houses built not adequately resistant to tornados can be strengthened with the CHMC. Chen et al. [7] conducted a set of impact tests on corrugated structural panels. The study showed how the impact location, impact velocity, and boundary condition can influence the impact response of corrugated structural panels.

^{*} Corresponding author.,

E-mail address: shafei@iastate.edu (D. Saini)

tion and energy saving advantages offered by SIPs. To evaluate the performance of SIPs subjected to windborne debris impact, there are limited studies available in the literature. Among them, Chen and Hao [10-12] investigated how the SIPs respond to impact-induced forces. It was found that the impact can cause large deformations in ductile metal skins, in contrast to localized deformation and damage in rigid skins, such as those made with OSB and fiber cement. In an effort to improve the impact resistance of SIPs, Meng et al. [13] investigated the use of glass fiber laminate for strengthening the SIPs with OSB face sheets. For example, adding a 3 mm glass fiber laminate was found to increase the strength against windborne debris impact by more than 75%. Jing et al. [14] explored the perforation resistance of sandwich panels with layered metallic cores. The layered structure was reported to adversely affect the performance during a projectile impact, as compared to monolithic sandwich panels. In a separate study focused on SIPs [15], it was observed that their energy absorption capacity can be 15%-100% greater than the sum of the capacities provided by their individual components. It was also determined that, although the impact resistance of the SIPs is primarily governed by the properties of face sheets, the density of the foam core can be an important factor. Despite the contribution of the past studies, none of them systematically evaluates the effects of face sheet and foam core properties on the response of SIPs subjected to debris impact. This has motivated the current study to address the gap in the state of the knowledge and practice concerning the performance of SIPs under windborne debris hazard.

In this study, a high-fidelity computational framework is developed to evaluate the structural vulnerability of SIPs with metal skins under windborne debris impact. This is achieved by developing a set of representative finite-element (FE) models for the SIPs calibrated with impact tests. To achieve a holistic assessment, more than 250 simulation cases are developed to properly understand the perforation resistance of the SIPs and the main factors contributing to it. This is ensured with appropriate material models, which include the strain rate effects and material erosion characteristics. Upon the validation of the developed FE models with the experimental test results, the main simulations are performed to determine the deformation pattern, critical and residual velocity, and energy absorption, which are later employed for evaluating the key design variables. The debris considered for the current study is a wood lumber with the impact velocities that range from 15 m/ s to 35 m/s, following the guide provided by the available codes and specifications [16-20]. The simulations are then extended to investigate the effects of a wide range of contributing factors, such as debris mass, impact velocity, and material and structural details of the face sheets and the foam core, on the overall performance of the SIPs during various windborne debris impact scenarios. For improving the design of this important category of composite wall panels, it is critical to determine their perforation resistance. Thus, a set of vulnerability curves are developed for the SIPs as a function of debris mass and velocity, capturing the complete penetration of debris into the SIPs, as the worst case scenario. This is expected to directly help with optimizing the material design and structural configuration of the SIPs used in the buildings exposed to the risk of wind and windborne debris hazard.

2. Modeling details

A set of explicit FE simulations are performed to evaluate the dynamic response of SIPs subjected to windborne debris impact. A detailed description of the geometry of the SIPs, material models, and loading scenarios is provided in this section.

2.1. Model setup

The SIPs available in the market have a constant width of 1.2 m. Their height, however, can vary to make sure that they properly fit in the building envelopes. In this study, the SIP specimens with the dimensions of 1.2 m \times 2.4 m and the core thickness of 100 mm are investigated (Fig. 1). The modeled SIPs represent the standard wall panels used in several residential and commercial buildings. The face sheets are made of 0.4 mm zincalume G300 steel, which is a continuous hot-dipped aluminum/zinc alloy-coated structural steel. The face sheets are modeled using fully integrated shell elements. The foam core is made of EPS, which has a high energy absorption capacity. The foam core is modeled using constant stress solid elements. In this study, the impact test requirements prescribed for extreme conditions, per Florida Building Code [17], are employed. This includes a lumber projectile with the nominal cross-sectional dimensions of 50 mm \times 100 mm (2 in. \times 4 in.) and a total mass of 4.0 kg. As observed in the past field surveys and experimental tests, the hardwood projectile commonly experiences no deformation or mass loss during windborne debris impact. Thus, it is modeled as a rigid object using constant stress solid elements. It should be noted that using a rigid material for the hardwood projectile neglects the elastic energy transferred to the timber projectile after impact [21]. This may produce a small overestimation of the energy dissipated by the SIPs, particularly for low impact velocities when rebounding of the projectile is likely. Since the velocities investigated in the current study correspond to the perforation level, this assumption was found to have no adverse effect on the accuracy of the simulation results.

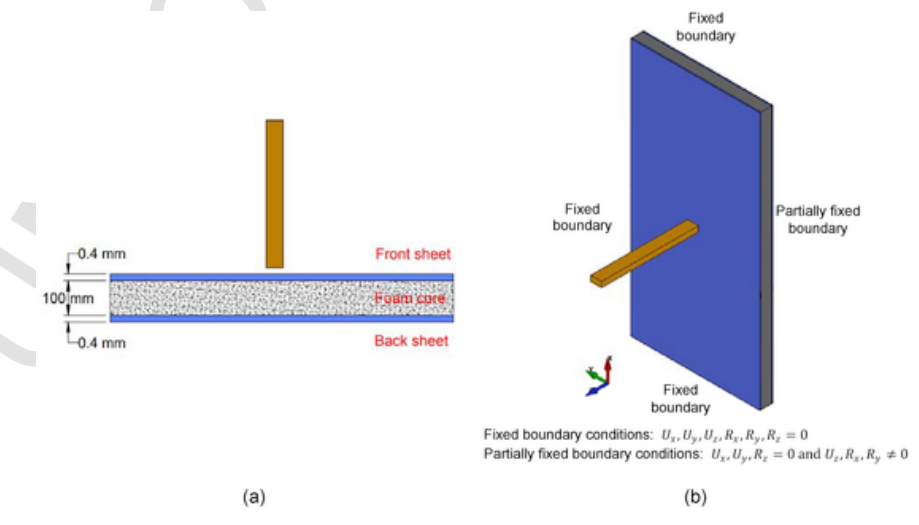


Fig. 1. (a) Details of the SIP test setup, and (b) FE model developed for the windborne debris impact simulations.

2.2. Material models

The material properties of the metal face sheets are described using the piecewise elastic-plastic material model that can capture the kinematic hardening plasticity [22–24]. Strain rate effects are incorporated into the model by using the Cowper-Symonds model [25] defined using the following equation:

$$\frac{\sigma_d}{\sigma_s} = 1 + \left(\frac{\dot{\varepsilon}}{C}\right)^{\frac{1}{p}} \tag{1}$$

Where σ_d is the dynamic flow stress at the strain rate of $\dot{\varepsilon}$; σ_s is the associated flow stress; and C and p are the Cowper-Symonds model parameters. In this study, C and p are assumed as 100 s⁻¹ and 10, respectively [11,26–28]. The elastic modulus and Poisson's ratio of the metal face sheets are 210 GPa and 0.3, respectively. Based on the stress-strain curve of zincalume G300 steel, a failure strain of 0.0525 is defined.

The EPS foam has a relatively complex behavior under external loads. The stress-strain curve of the EPS foam under compression can be broadly divided into three regions, i.e., elastic region, plateau compaction region, and densification region. It is important to note that the stress-strain relationship is dependent on the density of the EPS foam. The compressive elastic modulus and the yield strength both increase as the density increases. In this study, the modified crushable foam model is adopted to properly capture the main characteristics of the EPS foam used in the core of the SIPs. This model is an extension of the crushable foam model, which considers the yield stress as a function

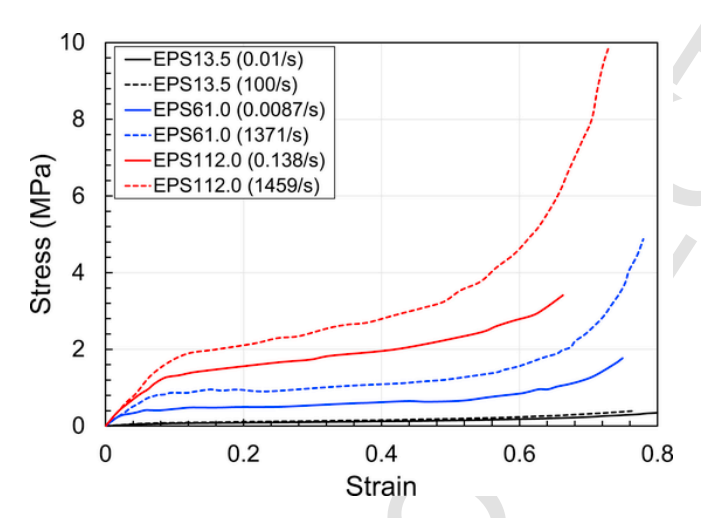


Fig. 2. Stress-strain curves (as a function of strain rate) for the three EPS foams investigated in the current study.

of volumetric strain and volumetric strain rate. The foam is assumed to be isotropic with the strain rate sensitivity captured using a stress versus volumetric strain relationship at various strain rates. Fig. 2 illustrates the stress-strain curve for the EPS foam at different strain rates. The EPS foam with a density of 13.5 kg/m³ is considered for the current study, replicating the foam commonly used in the building industry. The modeled foam has an elastic modulus of 900 kPa and a Poisson's ratio of 0.0001. To simulate damage formation and propagation, an erosion option with a shear strain failure criterion of 0.5 is employed for the EPS foam.

2.3. Boundary conditions and contact algorithms

To achieve accurate results, a proper modeling of boundary conditions is critical. In the current construction practice, each structural wall consists of several SIPs connected to each other. To reflect such connections, the SIPs are constrained against all the degrees of freedom at one vertical edge and partially fixed at the other edge (Fig. 1). The partial fixity involves constraints against in-plane translation and out-of-plane rotation. The top and bottom of the SIPs are fixed against all the degrees of freedom. The interactions between the SIP and the projectile, including friction effects, are controlled by using an eroding surface to surface contact with a segment-based contact option [29]. In addition, an eroding single surface contact is included to control the interaction between the face sheets and the foam core, as they experience damage. Since the EPS foam can undergo large deformations, an interior contact is defined to avoid negative volume within the core of the SIP. In the projectile tests performed on the SIPs, no debonding was observed between the face sheets and the foam core [11]. Therefore, a perfect bond is assumed between them in the current study.

3. Model validation and mesh convergence

The simulation setup is validated first with the experimental tests performed on the SIPs. The experimental tests included multiple projectile impacts on the SIPs that consisted of an EPS foam sandwiched between two steel face sheets with the dimensions of 0.76 m \times 1.20 m. The impact velocity ranged from 17 m/s to 26 m/s for these tests. The face sheets were made of zincalume G300 steel with a nominal thickness of 0.42 mm and a yield strength of 330 MPa. Three different thicknesses of the EPS foam with a density of 13.5 kg/m³ were used in the experiments [11]. The SIPs were mounted on a rectangular frame using G-clamps. A 4.0 kg hardwood projectile was launched using a pneumatically driven cannon (Fig. 3). To validate the developed FE models, a setup similar to that used for the experiments is developed in the LS-DYNA software package, including representative initial and boundary conditions. For the validation effort, a total of six tests are investigated with different core thicknesses and projectile impact velocities, as summarized in Table 1. It should be noted that upon validating the

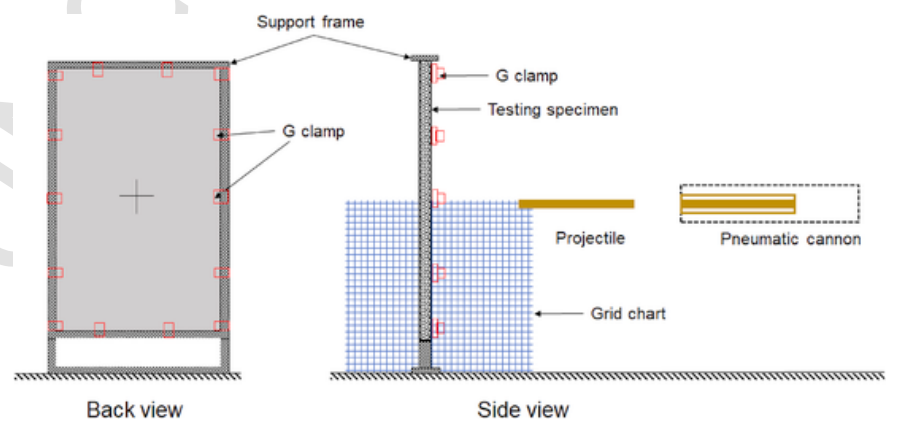


Fig. 3. Schematic diagram of experimental test setup replicated following [11].

Table 1Comparison of the simulation results with the experimental test data for the six SIP configurations tested for validation purposes

No.	Face sheet thickness (mm)	Core thickness (mm)	Dimension (m)	Debris mass (kg)	Initial velocity (m/s)	Residual velocity (m/s)		Perforation
						Experiment [11]	FE Simulation	
1	0.4	50	0.76 × 1.20	4.0	18	-3.8	-4.5	No
2	0.4	50	0.76×1.20	4.0	26	17.0	17.8	Yes
3	0.4	50	0.76×1.20	4.0	23	15.0	14.1	Yes
4	0.4	75	0.76×1.20	4.0	24	10.0	11.5	Yes
5	0.4	75	0.76×1.20	4.0	18	-4.0	-4.1	No
6	0.4	38	1.40×1.20	4.0	18	0.0	0.1	No

FE models with the first four tests, i.e., validation cases No. 1 through No. 4, the FE models are further tested using two additional tests, i.e., validation cases No. 5 and No. 6.

From each simulation, various structural response measures are extracted. Based on a review of the impacted SIPs, different modes of damage can be identified, ranging from the tearing of the front skin and core, but no complete penetration, to a full shear punching failure. For each specimen, the deformed shape and the residual velocity of the projectile are extracted for validation purposes. The residual velocity refers to the velocity of the projectile after complete perforation or rebound. A negative value for the residual velocity indicates that the projectile has rebounded after impact. According to Table 1, the residual velocities, as well as the penetration modes, are very much comparable with the experimental test results. The validation effort is further extended by comparing the out-of-plane displacements at two locations for the validation case No. 4, i.e., (1) half distance between the center and the long edge of the panel, and (2) half distance between the center and the short edge of the panel. For this case, the maximum out-of-plane displacements at the two locations are recorded to be 18.6 mm and 12.3 mm from the FE simulations, as compared to 18.9 mm and 11.4 mm measured in the experiments for the same locations, respectively. Further to capturing the maximum response measures, Fig. 4(a) shows how the post-impact deformed shape of the specimen investigated in the validation case No. 4 is compared between the FE simulation and the experimental test. The stress contours, in particular, successfully capture the creases formed in the front sheet consistent with the experiment. The validation case No. 5 involves a SIP with the dimensions of 0.76 m \times 1.20 m, including a foam core with a thickness of 75 mm. This SIP is impacted at the center with an impact velocity of 18 m/s, following the experimental test setup. The test data indicates that the debris rebounds with a velocity of 4.0 m/s after rupturing the front face sheet. The FE model is able to predict a very similar behavior, while capturing a rebound velocity of 4.1 m/s, consistent with the experiment. In the validation case No. 6, the SIP dimensions are 1.40 m \times 1.20 m with a core thickness of 38 mm. The SIP was impacted at the center with an impact velocity of 18 m/s. It is found that the debris pierces through but stays inside the SIP. The damage, in particular, is characterized by the rupture of the front face sheet followed by the tearing of the back skin. As shown in Fig. 4(b), such a behavior replicates the behavior recorded during the experimental test very well. This confirms that the calibrated FE models are satisfactory to simulate the perforation resistance of the SIPs under windborne debris impact.

Upon establishing the main model setup with the dimensions of $1.2~\mathrm{m} \times 2.4~\mathrm{m}$ and the core thickness of $100~\mathrm{mm}$, a mesh convergence analysis is conducted to determine an optimum mesh size. Considering the sensitivity of simulation results to the mesh size, a fine mesh size is required for the region of direct impact. Thus, three element sizes of $20~\mathrm{mm}$, $10~\mathrm{mm}$, and $5~\mathrm{mm}$ are tested for the two strips that pass through the impact location. Among the response measures of interest, the projectile is found to rebound after impacting the SIP with a mesh size of $20~\mathrm{mm}$. However, a perforation consistent with the experimental tests is observed for the mesh sizes of $10~\mathrm{mm}$ and $5~\mathrm{mm}$. From

the monitoring of the residual velocity, the mesh convergence is ensured by noting that the difference between the residual velocities obtained from the mesh sizes of 10 mm and 5 mm remains under 6%. Therefore, a mesh size of 5 mm is used for the two perpendicular strips, while the mesh size is increased to 20 mm in the rest of the SIP setup.

4. Results and discussion

Using the validated FE models, a set of impact simulations are conducted on the SIPs to evaluate their vulnerability to windborne debris impact. Various response measures, such as deformation pattern, critical and residual velocity, and energy absorption, are employed to quantify the structural performance of the SIPs subjected to a range of debris impact velocities. Fig. 5 illustrates the damage formed in the SIPs under the increasing impact velocities of 15 m/s, 20 m/s, and 25 m/s. The SIP does not experience perforation under 15 m/s. However, perforation occurs at 20 m/s and 25 m/s impact velocities with a punching shear mode of failure. It is interesting to note that with increasing the impact velocity from 20 m/s to 25 m/s, the damaged area slightly decreases. This can be explained by the fact that the portion of the panel that can contribute to resisting the impact force is reduced in the absence of sufficient response time due to the increased impact velocity. The impact process is further explained by investigating the energy absorption and critical velocity of the SIPs under consideration.

4.1. Energy absorption

The amount of energy absorbed during impact can be used as a measure to evaluate the participation of various components of the SIPs in resisting the impact load. By considering each numerical simulation as a closed system, the total energy of the system must remain constant. The kinetic energy introduced by the impacting debris is partly absorbed by the SIP. The absorbed energy is due to either material damage (E_{damage}) or structural deformation $(E_{deformation})$. While the former is characterized by the process of erosion, the latter is represented by the changes in the internal energy. Fig. 6 shows the amount of energy absorbed by the front sheet, foam core, and back sheet at the impact velocities of 15 m/s, 20 m/s, and 25 m/s. The absorbed energy is presented as the fraction of the total energy imparted to the panel. Under an impact velocity of 15 m/s, the SIP absorbs 100% of the total energy with the primary contribution of the foam core, which receives more than 80% of the total energy. The fraction of impact energy absorbed by the SIP drops to 84% and 56% for the impact velocity of 20 m/s and 25 m/s, respectively. This can be explained by the fact that the projectile continues moving with a residual velocity of 8.32 m/s and 16.01 m/s after full penetration, respectively. Reviewing the contribution of the front and back sheets, it is observed that the front sheet absorbs a higher fraction of the applied energy when the timber projectile rebounds. However, the amount of energy absorbed by the back sheet becomes equal to the front sheet when perforation occurs. The energy absorption characteristics are further explored by evaluating the ratio of $E_{damage}/E_{deformation}$. Fig. 7 illustrates the relationship between E_{damage} and $E_{deformation}$ for the three impact velocities of 15 m/s, 20 m/

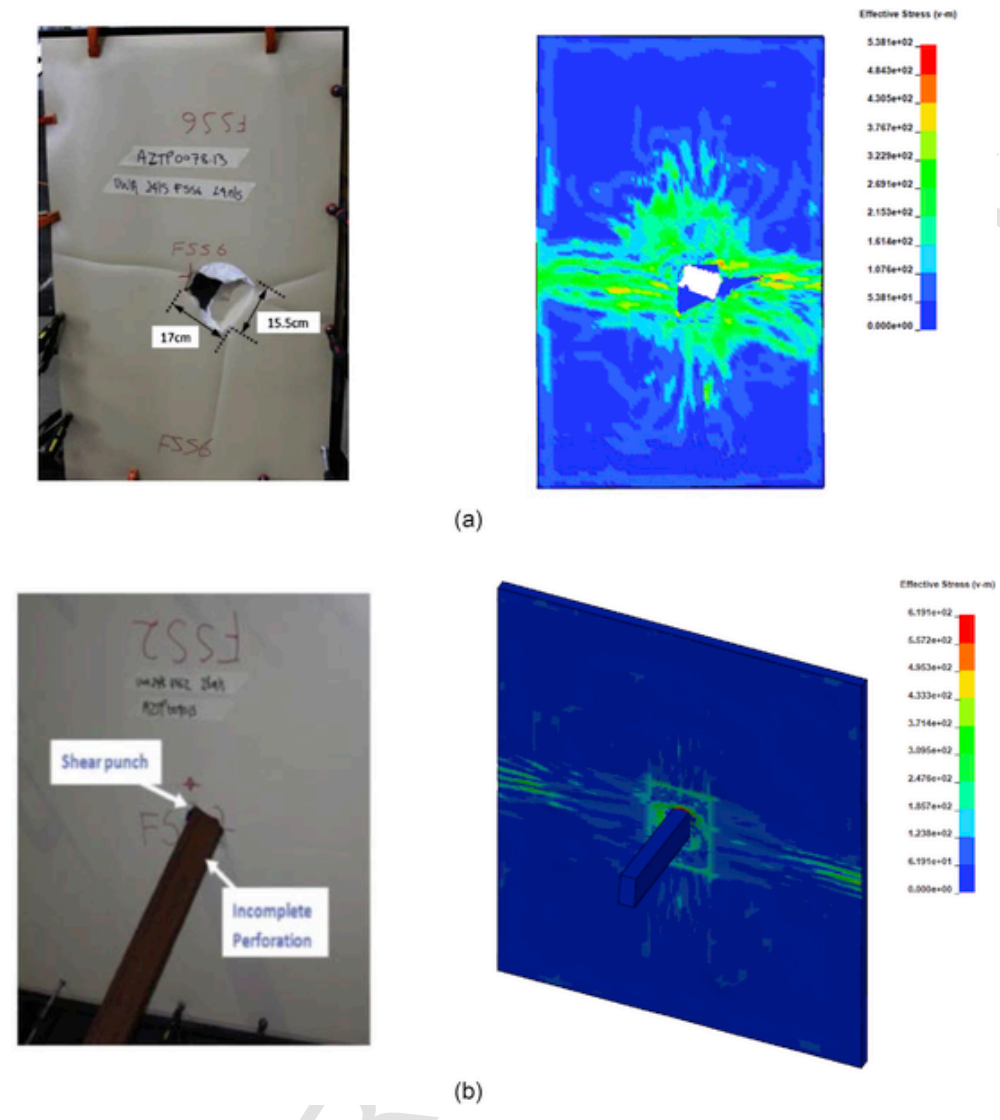


Fig. 4. Comparison of the post-impact deformed shapes obtained from the experimental tests [11] and FE simulations: (a) validation case No. 4, and (b) validation case No. 6.

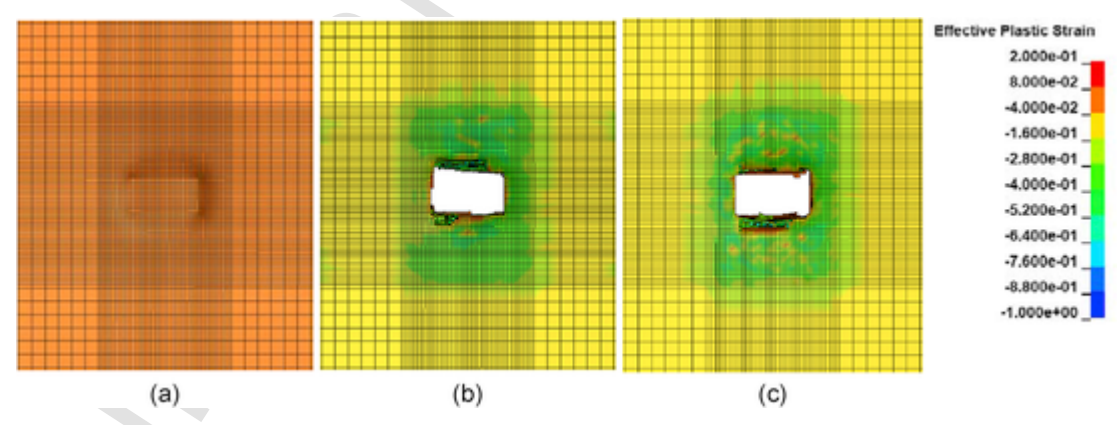


Fig. 5. Damage patterns in the SIPs under the three impact velocities of (a) 15 m/s, (b) 20 m/s, and (c) 25 m/s.

s, and 25 m/s. For the impact velocity of 15 m/s, the SIP does not experience any material damage, i.e., $E_{damage} = 0$, and all the energy dissipation occurs due to deformations, which naturally include indentations as well. However, with increasing the impact velocity, E_{damage} consistently increases due to the increase in the extent of damage, result-

ing in an increase in the ratio of $E_{damage}/E_{deformation}$. One important observation is that the ratio of $E_{damage}/E_{deformation}$ is higher for the front sheet than for the back sheet and the foam core. This further highlights the role of the front sheet to resist the impact-induced forces.

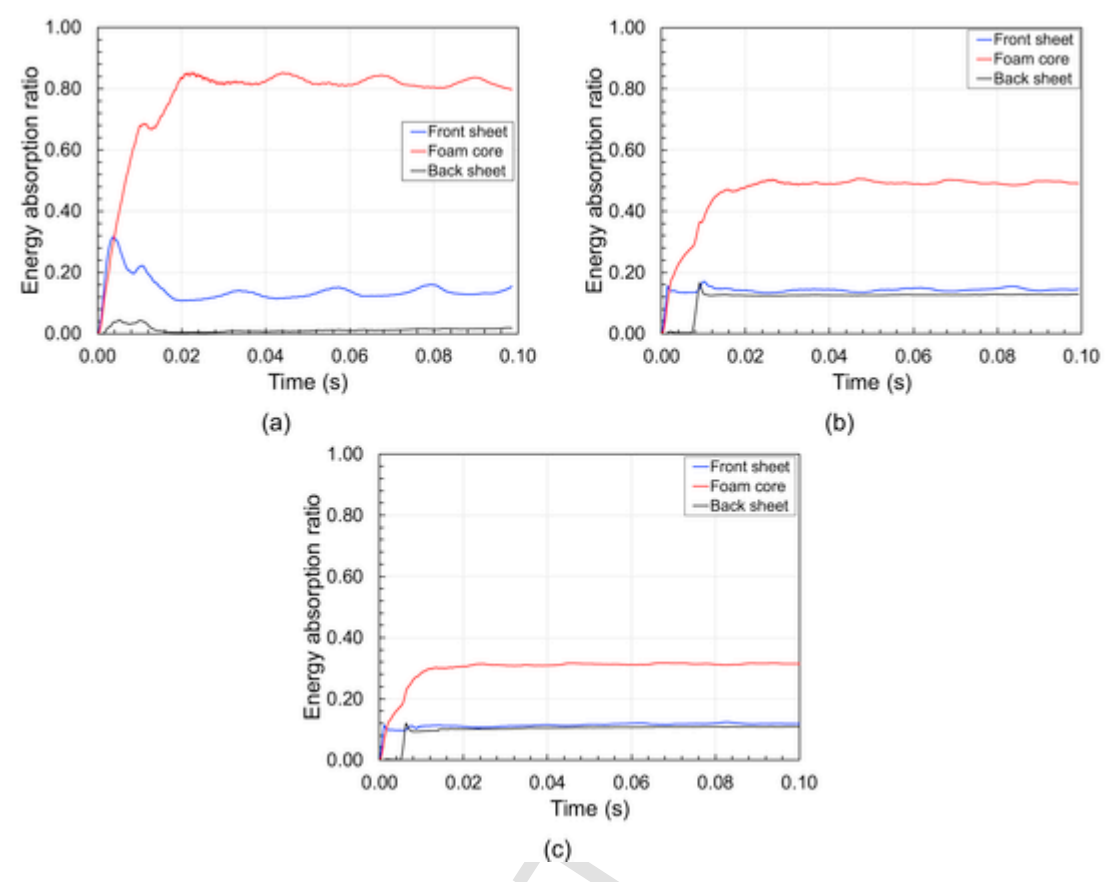


Fig. 6. Time-histories of the fractions of the total impact energy absorbed by the main SIP components under an impact velocity of (a) 15 m/s, (b) 20 m/s, and (c) 25 m/s.

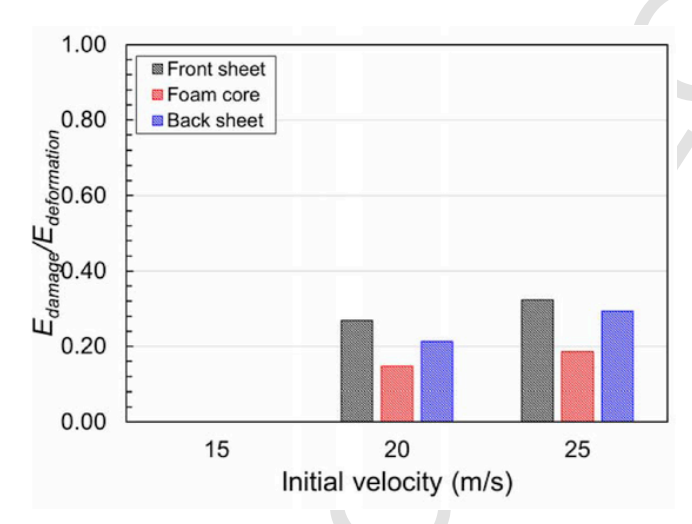


Fig. 7. Relationship between E_{damage} and $E_{deformation}$ under three impact velocities.

4.2. Critical velocity

The critical velocity is defined as the minimum impact velocity required for the windborne debris object to perforate through the SIP. The critical velocity for a particular configuration of SIP can be determined from the FE simulations by having a number of trials to determine the impact velocity needed for the debris to penetrate into the SIP with zero residual velocity. Considering the importance of this velocity and the computational effort required to capture it, an alternative approach is employed in the current study by performing curve fitting

on the residual velocity data points to predict the critical velocity. After recording the residual velocities from a set of FE simulations with increasing initial debris impact velocities, the following expression proposed by Ipson and Recht [30] is used to relate the initial, v_i , residual, v_r , and critical velocity, v_c , of the windborne debris object:

$$v_r = \begin{cases} 0 & 0 \le v_i \le v_c \\ a(v_i^P - v_c^P)^{1/P} & v_i > v_c \end{cases}$$
 (2)

Where P is a coefficient that can be assumed equal to 2 for a rigid debris; and a is a coefficient that can be approximated using the following expression:

$$a = \frac{m_d}{m_t + m_d} \tag{3}$$

Where m_d and m_t are the mass of the windborne debris object and the mass of the target ruptured by the debris, respectively. Fig. 8 shows how Equations (2) and (3) can be utilized to fit a curve to the residual velocities extracted from the FE simulations for the initial impact velocities, ranging between 20 m/s and 35 m/s. With the developed equations, a critical velocity of 17.47 m/s is predicted for the SIP under consideration. This is found completely consistent with the critical velocity determined directly from the numerical simulations (as shown in Fig. 8 by a blue dot).

5. Investigation of contributing design factors

A comprehensive investigation of the structural details, material properties, and impact intensities that immediately influence the performance of the SIPs subjected to windborne debris hazard is conducted in the current study to obtain a proper insight for an optimal design of this important category of building envelope components.

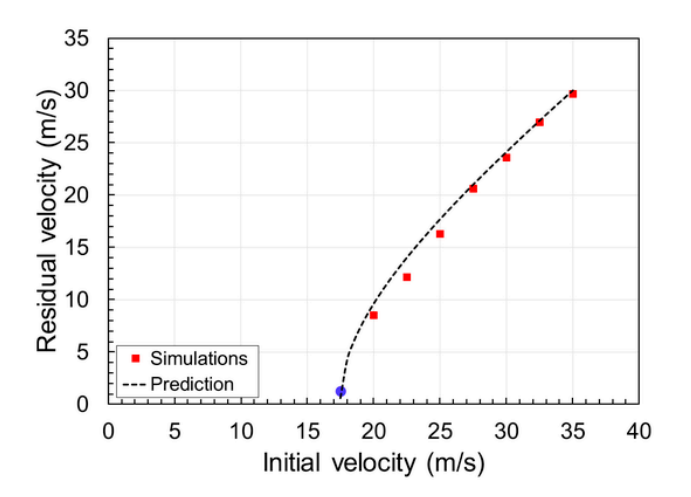


Fig. 8. Relationship between the residual and initial impact velocities to determine the critical velocity for the SIPs under consideration.

5.1. Thickness of metal sheets

The perforation resistance of the SIPs greatly depends on the thickness of their metal sheets, especially the front one, which is directly impacted by windborne debris objects. To evaluate this design parameter, five front sheet thicknesses ranging from 0.4 mm to 0.8 mm (with 0.1 mm intervals) are considered. All the SIPs are assumed to have a similar steel yield strength of 330 MPa, EPS core thickness of 100 mm, and EPS density of 13.5 kg/m³. Under various impact velocities, i.e., from 17.5 m/s to 35 m/s with 2.5 m/s intervals, the simulations are performed and the main structural response measures are extracted. Fig. 9(a) shows the predicted residual velocity curves for the five front sheet thicknesses. A significant decrease in the residual velocity is observed with increasing the front sheet thickness from 0.4 mm to 0.5 mm and from 0.5 mm to 0.6 mm. With further increasing the thickness, however, reduction in the residual velocity becomes less pronounced. Fig. 9(b) illustrates the critical velocities for various front sheet thicknesses. An increase of 21% and 9% are observed when increasing the front sheet thickness from 0.4 mm to 0.5 mm and from 0.5 mm to 0.6 mm, respectively. Similar to the residual velocity, the effect of the front sheet thickness becomes marginal if the thickness is increased beyond 0.6 mm. This can be further explained by recording the energy absorbed by various components of the SIPs with different front sheet thicknesses.

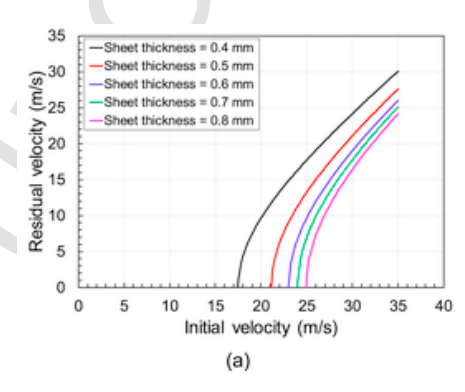
Fig. 10 presents the energy absorbed by the three components of the SIPs under an impact velocity of 20 m/s. With increasing the front sheet thickness from 0.4 mm to 0.8 mm, it is observed that the energy absorbed by the front sheet increases, while the energy absorbed by the back sheet decreases. This highlights that a reduced thickness can

be considered for the back sheet when the front sheet can withstand the impact load. The energy absorbed by the foam core is found to increase by up to 32% with increasing the front sheet thickness from 0.4 mm to 0.7 mm. This can be explained through the load transfer observed in the impacted SIPs. A higher front sheet thickness results in a wider transfer of the impact force to the foam core, as the front sheet does not experience immediate perforation. Thus, the foam core experiences larger deformations and higher energy absorption. With further increasing the front sheet thickness from 0.7 mm to 0.8 mm, however, the energy absorbed by the foam core drops by 4%. This can be attributed to the high resistance of the 0.8 mm front sheet against debris impact. This is evident in the drop of the energy absorbed by the back sheet as well.

Noting the importance of the front sheet thickness to resist (and distribute) the impact forces, the effect of utilizing unequal thicknesses for the front and back sheets is explored by considering asymmetric thicknesses (rather than the conventional symmetric ones). For this purpose, three different SIP configurations are considered with varying face sheet thicknesses, while maintaining a constant total thickness for the front and back sheets. The configurations under consideration are (i) 0.4 mm thickness for each of the front and back sheets, (ii) 0.2 mm thickness for the front sheet and 0.6 mm thickness for the back sheet, and (iii) 0.6 mm thickness for the front sheet and 0.2 mm thickness for the back sheet. Fig. 11 shows the debris velocity time histories for three SIP configurations under initial impact velocities of 20 m/s and 25 m/s. It is observed that the asymmetric face sheets have a significant influence on lowering the residual velocity (up to 38%) for the initial velocity of 20 m/s. However, no significant influence is observed on the residual velocities as the impact velocity increases to 25 m/s. This is an indicator that the use of asymmetric face sheets is most effective in the range of velocities close to the critical velocity.

5.2. Material properties of metal sheets

Choosing metal sheets with appropriate material properties is critical to ensure a satisfactory performance of SIPs. This can be primarily captured through considering the yield strength and failure strain of the metal sheets. In the current study, four yield strengths of 330 MPa, 440 MPa, 550 MPa, and 660 MPa are investigated. The SIPs have a core thickness of 100 mm and an EPS density of 13.5 kg/m³. Fig. 12(a) shows the residual velocities obtained for the windborne debris objects that impact the SIPs of different yield strengths. A decrease in the residual velocities is observed with the increase of the vield stress of the metal sheets. However, the difference in the residual velocities reduces as the impact velocity increases. As expected, the SIPs that have metal sheets with a higher yield strength exhibit a better performance. This is due to the reduction in the induced strains, and consequently, deformations, as the yield stress increases. A significant reduction in the residual velocities is observed when the yield strength is increased from 330 MPa to 440 MPa. With further increasing the yield stress to 660 MPa, however, this reduction slows down. In terms of crit-



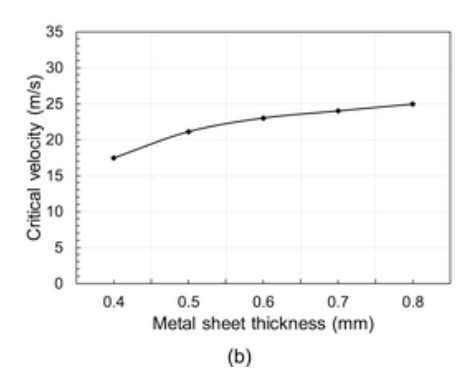


Fig. 9. Effect of the front sheet thickness on the perforation resistance of SIPs: (a) residual velocity, and (b) critical velocity.

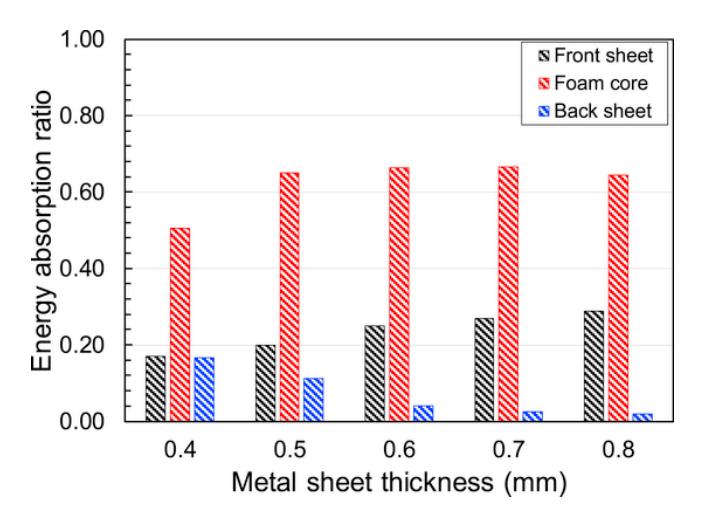


Fig. 10. Effect of the front sheet thickness on the energy absorption of the three different components of the SIPs.

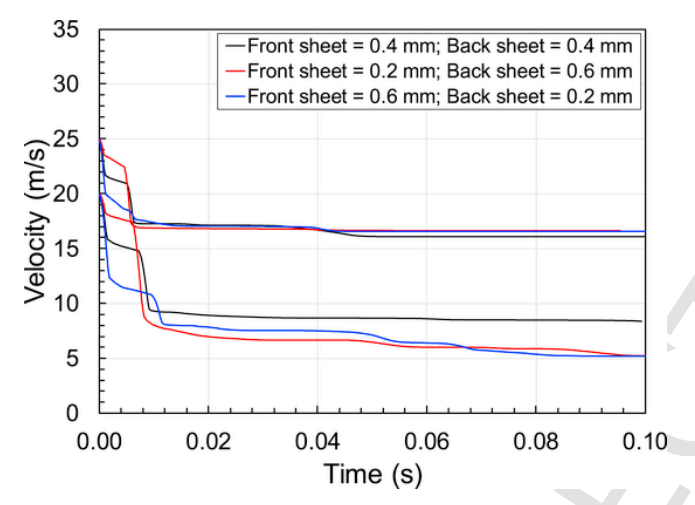


Fig. 11. Debris velocities recorded after impact to the SIPs of various front and back sheet thicknesses.

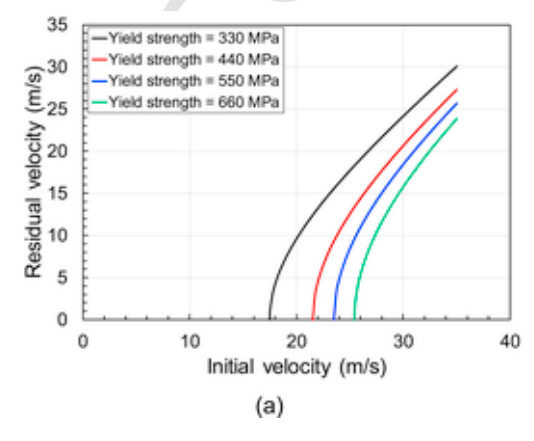
ical velocity, a critical velocity of 17.47 m/s is obtained for the yield strength of 330 MPa in contrast to 21.55 m/s for the yield strength of 440 MPa. With further increasing the yield strength to 550 MPa and 660 MPa, the critical velocity increases to 23.50 m/s and 25.43 m/s, respectively. This trend can be further understood by investigating the energy absorption of the SIP components. Fig. 12(b) illustrates the effect of the yield strength of the metal sheets on the energy absorbed

by the three components of the SIP at an impact velocity of 20 m/s. With increasing the yield strength from 330 MPa to 660 MPa, the energy absorbed by the foam core increases by 83%. This results in a 90% drop in the energy absorbed by the back sheet.

Metal sheets can exhibit variations in their fracture strain, leading to changes in the perforation resistance of the SIPs. To study this parameter, three fracture strains of 0.0525, 0.0600, and 0.0675 are selected. The SIPs are assumed to have a yield strength of 330 MPa, an EPS core thickness of 100 mm, and an EPS density of 13.5 kg/m³. Fig. 13(a) shows the residual velocities of the windborne debris objects, impacting the SIPs of three different fracture strains. Contrary to the yield strength. the fracture strain does not have a significant effect on the residual velocities. With increasing the fracture strain from 0.0525 to 0.0675, the critical velocity increases by 12%. The critical velocity also experiences a marginal increase by observing 17.47 m/s, 18.75 m/s, and 19.65 m/s for the fracture strains of 0.0525, 0.0600, and 0.0675, respectively. This is further explored by evaluating the energy absorption of the SIPs with various fracture strains considered for the metal sheets. Fig. 13(b) presents the effect of fracture strain on the energy absorbed by the three components of the SIPs at an impact velocity of 20 m/s. It can be seen that increasing the fracture strain does not cause any notable effect on the distribution of the absorbed energy. With increasing the fracture strain from 0.0525 to 0.0675, the energy absorbed by the front sheet, foam core, and back sheet is found to increase by 28%, 13%, and 17%, respectively.

5.3. EPS core foam properties

The density of the EPS foam can significantly affect the elastic compressive modulus and the yield strength of the core of SIPs, leading to changes in their perforation resistance. To evaluate this important parameter, three EPS core densities of 13.5 kg/m³, 61.0 kg/m³, and 112.0 kg/m³ are considered. The elastic modulus of these three foams are assumed as 0.9 MPa, 24.0 MPa, and 55.0 MPa, respectively [31,32]. Fig. 14 presents the stress contours in the SIP for the three EPS core densities under the impact velocity of 20 m/s. It is clear that increasing the EPS density significantly reduces the amount of damage to the SIP. At the EPS density of 13.5 kg/m³, the projectile completely penetrates through the panel, whereas the SIPs with the EPS densities of 61.0 kg/m³ and 112.0 kg/m³ are found strong enough to resist the projectile impact, despite the rupture of the front sheet. The effect of the EPS core density is further explained by comparing the energy absorbed by the SIPs at an impact velocity of 20 m/s. As shown in Fig. 15(a), the energy absorbed by the foam core consistently increases with increasing the density, while the energy absorbed by both front and back sheets reduce. With increasing the EPS foam density from 13.5 kg/m³ to 112.0 kg/m³, the energy absorbed by the front sheet and back sheet decreases by 43% and 87%, respectively. This reduction



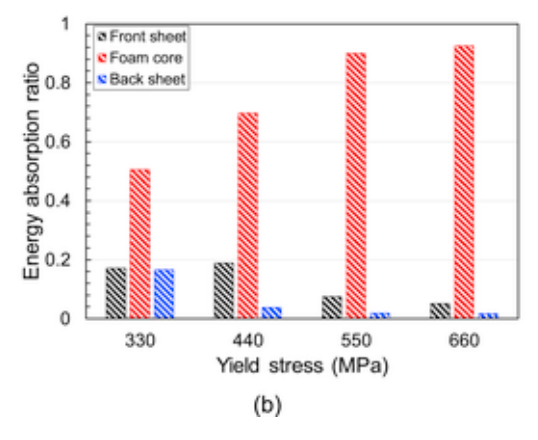


Fig. 12. Effect of the yield strength of metal sheets: (a) residual velocity curves, and (b) energy absorption.

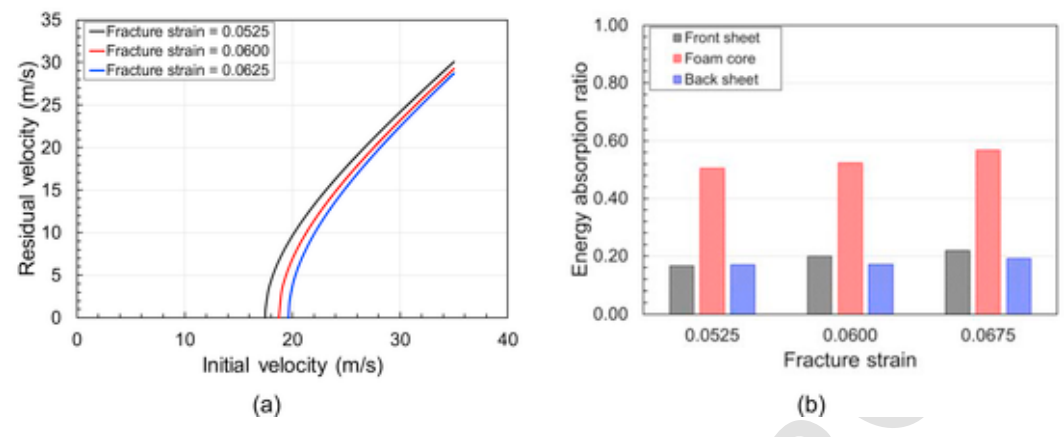


Fig. 13. Impact response of the SIPs with various fracture strains considered for the metal sheets: (a) residual velocity curves, and (b) energy absorption.

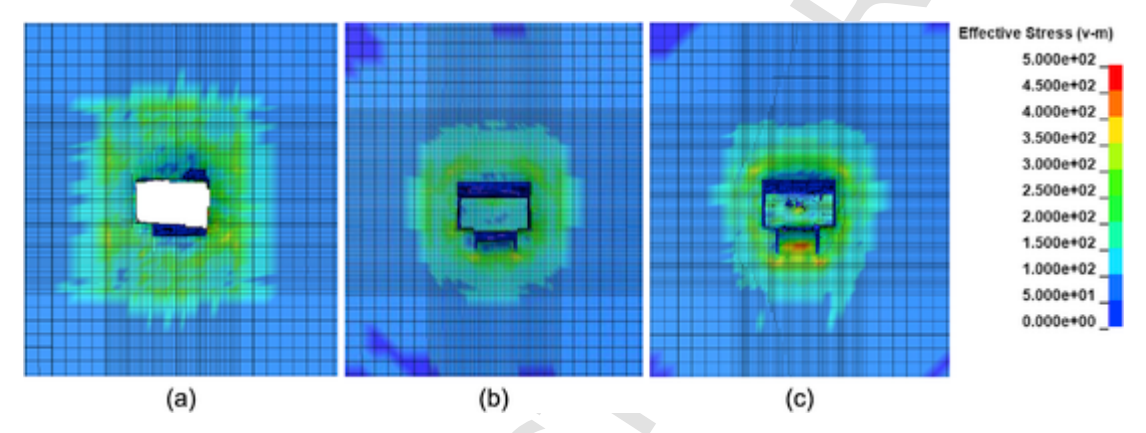


Fig. 14. Stress contours of the SIPs with the three different core densities of (a) 13.5 kg/m^3 , (b) 61.0 kg/m^3 , and (c) 112.0 kg/m^3 .

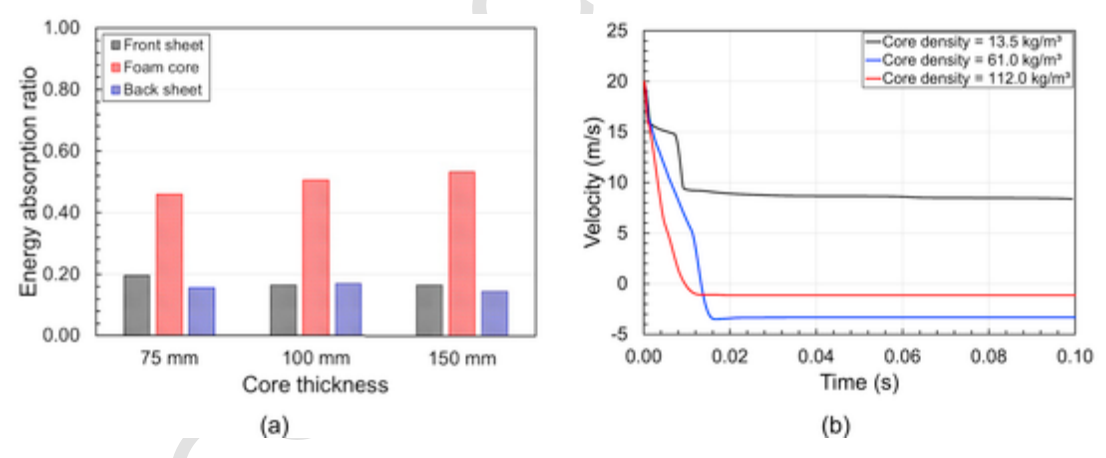


Fig. 15. Response of the SIPs with three different core densities: (a) energy absorption, and (b) velocity time histories.

in the energy absorption of the face sheets is compensated by a 74% increase in the energy absorbed by the EPS foam core. This can be further supported by reviewing the residual velocity profiles, as shown in Fig. 15(b). In this figure, the debris penetration through the front sheet is characterized by the first change in the slope of the velocity line. The second change in the slope of the velocity line marks the debris penetration through the back sheet. According to the velocity profiles, the SIPs with the core densities of $61.0~{\rm kg/m^3}$ and $112.0~{\rm kg/m^3}$ do not undergo full perforation, as the debris is found to rebound. For the core density of $13.5~{\rm kg/m^3}$, however, the front sheet is punched through when the debris velocity is $15.86~{\rm m/s}$, followed by a full penetration when the residual debris velocity is $9.29~{\rm m/s}$.

The EPS foam thickness is another parameter that can affect the perforation resistance of SIPs. In this study, three core thicknesses of 75 mm, 100 mm, and 150 mm are considered. The SIPs have a steel yield strength of 330 MPa and an EPS density of 13.5 kg/m³. Fig. 16(a) compares the energy absorbed by the three components of the SIPs. Energy absorbed by the EPS core increases from 46% to 53% of the total energy with increasing the thickness from 75 mm to 150 mm. However, the amount of energy absorbed by the front and back sheets do not change significantly. This observation is further justified using the velocity profiles obtained for various core thickness under the impact velocity of 20 m/s. As shown in Fig. 16(b), although the front sheet is penetrated at the same velocity of 15.86 m/s, the velocity at which the back sheet undergoes failure is lowered by 15% with increas-

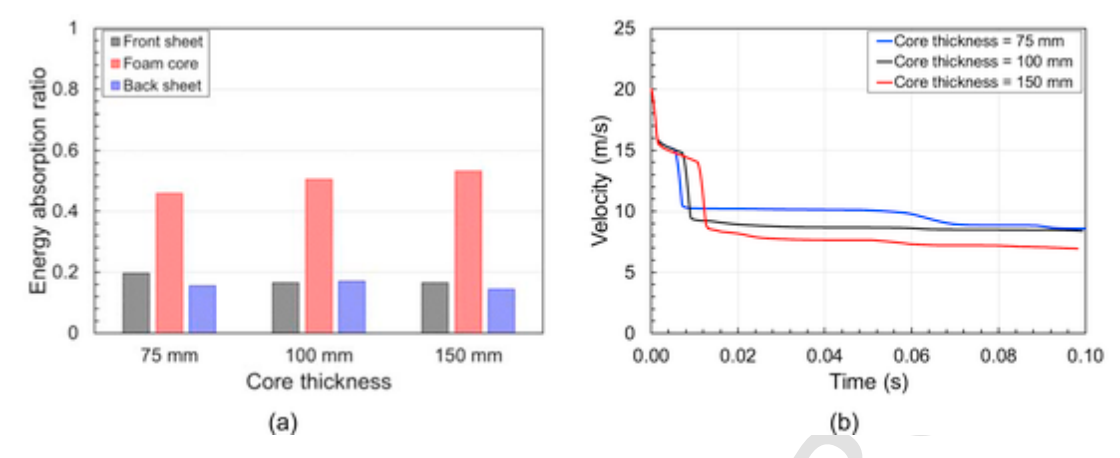


Fig. 16. Effect of the foam core thickness on the response of SIPs: (a) energy absorption ratio, and (b) velocity time histories.

ing the core thickness from 75 mm to 150 mm. Further to delaying the time of penetration, it is observed that the residual velocity decreases from 8.59 m/s to 6.92 m/s with increasing the core thickness from 75 mm to 150 mm. This highlights the contribution of the foam core to providing the expected resistance against perforation and subsequent damage.

6. Vulnerability assessment

During strong windstorms, the mass of debris flown by the wind can vary from the standard mass prescribed by the current guidelines and specifications [16,17,19]. To broaden the scope of investigations performed in the current study, a range of windborne debris masses are considered beginning from 2.0 kg to 8.0 kg in 2.0 kg intervals. The SIPs have a steel yield strength of 330 MPa, an EPS core thickness of 100 mm, and an EPS density of 13.5 kg/m³. Fig. 17(a) shows how the residual velocities are influenced as a function of initial impact velocity. The residual velocities are found to decrease with increasing the mass of the impacting object. However, the effect of mass on the residual velocities becomes less pronounced with increasing the mass to 8.0 kg. As shown in Fig. 17(b), the critical velocity for 8.0 kg debris mass is determined to be 26% lower than the critical velocity for 4.0 kg debris mass. On the other hand, the critical velocity is found to be 50% higher for the 2.0 kg debris mass than that for the 4.0 kg debris mass. The relationships obtained for the debris impact characteristics can be expressed in the form of vulnerability curves. The SIPs undergo perforation when the combination of debris mass and velocity falls above the curve, while they will be safe when this combination falls below the curve.

To facilitate the design of new and assessment of existing SIPs exposed to the windborne debris hazard, a set of vulnerability curves

are developed for the main SIP configurations considered in the current study. Based on the holistic matrix of the performed FE simulations, it is found that the front sheet thickness, steel yield strength, and foam core density have the most significant effects on the response of SIPs to debris impact. Fig. 18(a) presents the vulnerability curves for the SIPs with the front sheet thicknesses of 0.4 mm, 0.6 mm, and 0.8 mm. On the other hand, Fig. 18(b) illustrates the vulnerability curves as a function of yield strength of metal sheets, ranging from 330 MPa to 660 MPa. For both front sheet thickness and yield strength of steel, the change of the critical velocity as a function of mass is found to be consistent, while the effect of debris mass diminishes when approaching the masses above 6.0 kg. Fig. 18(c) presents the vulnerability curves as a function of the EPS foam core density. For a windborne debris mass of 4.0 kg, the critical velocity increases by 20% with increasing the density from 13.5 kg/m³ to 61 kg/m³. The effect of density becomes more pronounced as the density is further increased to 112 kg/m³. For the foam density of 112 kg/m³, the critical velocity is found to be 52% higher than that recorded for the SIP with a core density of 13.5 kg/m³. Similar trends of critical velocity are observed for the windborne debris masses of 2.0 kg, 6.0 kg, and 8.0 kg. Such vulnerability curves are anticipated to serve as a practical aid for the design and assessment of composite SIPs subjected to windborne debris impact.

7. Conclusions

The structural response and perforation resistance of the SIPs were investigated under windborne debris impact. Upon validating the developed FE models with the experimental test results, the performance of various SIPs was examined by evaluating their deformation pattern, critical and residual velocity, and energy absorption. The simulations were then extended to study the main design factors, including

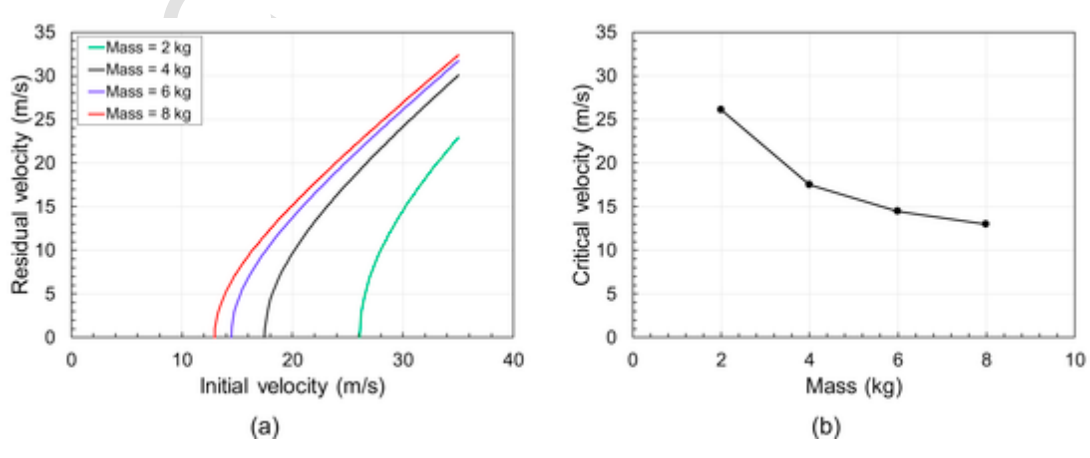


Fig. 17. Effect of the windborne debris mass on: (a) residual velocities, and (b) critical velocities.

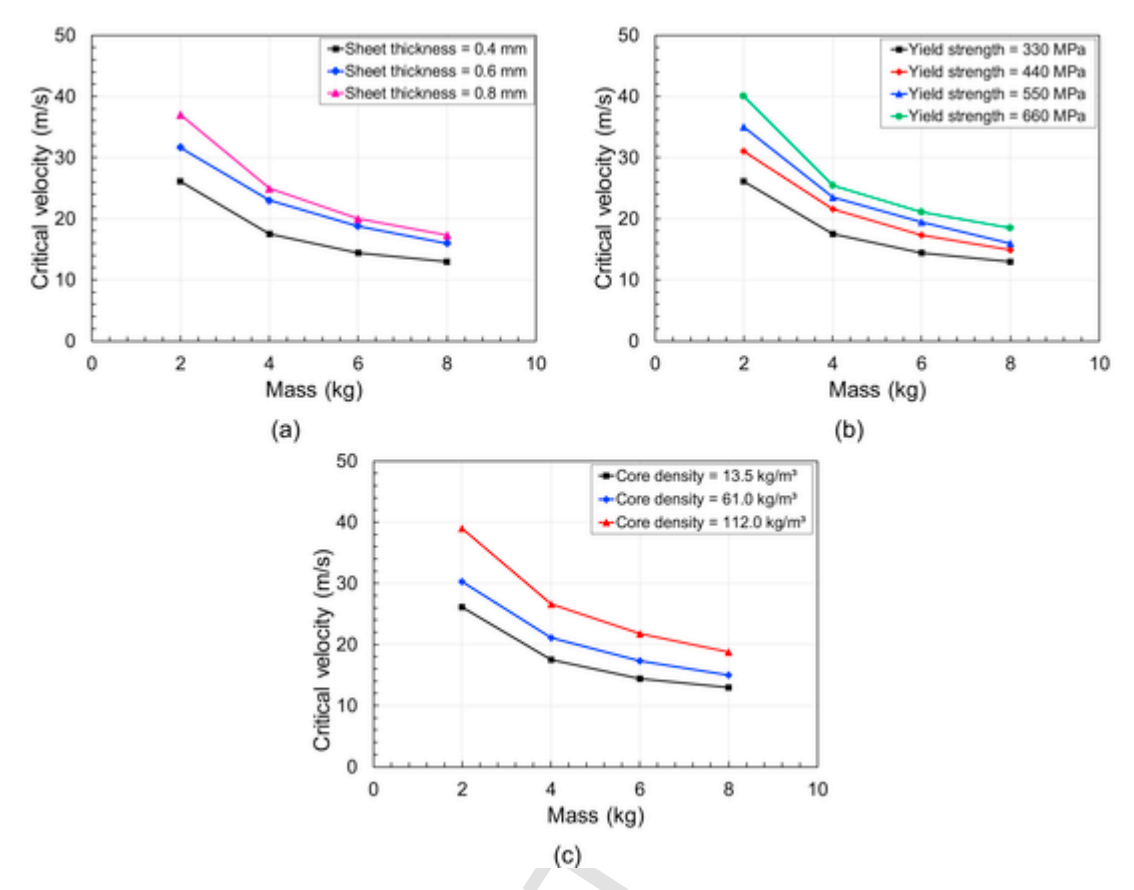


Fig. 18. Vulnerability curves developed for evaluating the perforation resistance of the SIPs as a function of: (a) front sheet thickness, (b) steel yield strength, and (c) foam core density.

the structural details and material properties of both metal sheets and the foam core. The main observations and findings can be summarized as follows:

- The energy absorption of the SIPs was quantified to evaluate the contribution of their various components. The energy absorption process revealed that 50%–90% of the total energy is often absorbed by the foam core. In addition to energy absorption, the critical velocity was predicted as the minimum impact velocity required for the windborne debris to perforate through the SIP. This was achieved through developing the necessary relationship between the initial impact and residual velocities. Further to saving the computational effort, it was found that the predicted critical velocities are in a complete agreement with those extracted directly from the FE simulations.
- The performance of the SIPs subjected to windborne debris impact was found to be enhanced by increasing the front sheet thickness, steel yield strength, and steel fracture strain. This was attributed to improving the transfer of impact-induced forces from the front sheet to the foam core and back sheet. With increasing the front sheet thickness from 0.4 mm to 0.8 mm, the critical velocity increased by 43%. On the other hand, the critical velocity increased by 46% with increasing the yield strength of the front sheet from 330 MPa to 660 MPa. Fracture strain of the steel used in the front sheet was observed to have only a marginal positive effect on the impact resistance of the SIPs (compared to thickness and yield strength).
- The effect of asymmetric face sheet thicknesses was explored on the perforation resistance of SIPs. Three different values of face sheet thicknesses were investigated, while the total thickness of the front and back sheets was kept the same for all the three cases. The simulation results indicated that asymmetric face sheets can have a significant effect on the response of the SIPs when they are subjected to the impact velocities close to their critical velocity. However, the ef-

- fect on the residual velocity was found to diminish with increasing the impact velocity further.
- The perforation resistance of the SIPs was significantly improved with adding to the density of the foam core. This was attributed to the fact that the foam core absorbs significantly more energy than the metal face sheets. Consistent with this observation, the critical velocities for the SIPs with the foam core densities of 61 kg/m³ and 112 kg/m³ were found to be 20% and 52% higher than the SIPs with the foam core density of 13.5 kg/m³. On the other hand, increasing the core thickness caused more energy to be absorbed by the foam core, while reducing the energy received by the back sheet. Overall, however, an increase in the core thickness resulted in a marginal improvement in the perforation resistance. This was quantified by an 11% increase in the critical velocity when the core thickness was changed from 100 mm to 150 mm.
- A set of vulnerability curves for the SIPs were developed, capturing the risk of failure of this important category of wall panels under the windborne debris hazard. The developed curves are a function of mass and critical velocity of the impacting debris and can be used as a practical aid to identify the impact scenarios that can cause perforation in the SIPs. This provides the building industry with an in-depth insight for the optimal design of SIPs in the regions prone to windborne debris hazard. If properly designed, the SIPs can not only withstand debris impacts with only minor to no damage, but also offer an economic choice for durable and energy-efficient wall panels.

CRediT authorship contribution statement

Dikshant Saini: Methodology, Software, Validation, Investigation, Writing - original draft. **Behrouz Shafei:** Conceptualization, Methodology, Investigation, Writing - review & editing, Funding acquisition, Supervision.

Declaration of competing interest

The authors declare that they have no known competing financial interests or personal relationships that could have appeared to influence the work reported in this paper.

Acknowledgement

The research study, the results of which reported in this paper, was partially sponsored by the National Science Foundation under Grants No. 1826356 and 1827774. The authors would like to acknowledge the sponsor for this support. Opinions, findings, and conclusions expressed in this paper are of the authors and do not necessarily reflect those of the National Science Foundation.

References

- [1] What is Expanded Polystyrene (Eps) foam? The possibilities are endless! Web Addressaccessedhttps://insulationcorp.com/eps/6 April 2019
- [2] D Thompsett, A Walker, R Radley, B Grieveson Design and construction of expanded polystyrene embankments: practical design methods as used in the United Kingdom. Construct Build Mater 1995;9:403–411.
- [3] U Frye, J Ginger, P Mullins Response of cladding to windborne debris impact. Wind Eng. Taipei, Taiwan Chinese Assoc. Wind Eng.; 2009. seventh Asia--Pacific Conf.
- [4] H Zhou, K Dhiradhamvit, T L Attard Tornado-borne debris impact performance of an innovative storm safe room system protected by a carbon fiber reinforced hybrid polymeric-matrix composite. Eng Struct 2014;59:308–319.
- [5] A H Herbin, M Barbato Fragility curves for building envelope components subject to windborne debris impact. J Wind Eng Ind Aerod 2012;107:285–298.
- [6] D Saini, B Shafei Vulnerability of metal roof decking systems subjected to windborne debris impact. FL: 5th Am. Assoc. Wind Eng. Work. Miami; 2018.
- [7] W Chen, H Hao, H Du Failure analysis of corrugated panel subjected to windborne debris impacts. Eng Fail Anal 2014;44:229–249.
- [8] D L Scheer Large wind missile impact performance of public and commercial building assemblies. Tallahassee, Florida: Florida State University; 2005.
- [9] S T Peters, I N Robertson The effects of windborne debris on saferoom wall panels and fenestration systems. Research report UHM/CEE/12-10. Manoa: University of Hawaii; 2012.
- [10] W Chen, H Hao, J Li Fragility curves for corrugated structural panel subjected to windborne debris impact. Int. Conf. Performance-based Life-cycle Struct. Eng. 2015;877–883.
- [11] W Chen, H Hao Experimental and numerical study of composite lightweight structural insulated panel with expanded polystyrene core against windborne debris impacts. Mater Des 2014;60:409–423.

- [12] W Chen, H Hao Performance of structural insulated panels with rigid skins subjected to windborne debris impacts--Experimental investigations. Construct Build Mater 2015;77:241–252.
- [13] Q Meng, H Hao, W Chen Laboratory test and numerical study of structural insulated panel strengthened with glass fibre laminate against windborne debris impact. Construct Build Mater 2016;114:434–446.
- [14] L Jing, F Yang, L Zhao Perforation resistance of sandwich panels with layered gradient metallic foam cores. Compos Struct 2017;171:217–226.
- [15] W K Shih, B Z Jang Instrumented impact testing of composite sandwich panels. J Reinforc Plast Compos 1989;8:270–298.
- [16] NRC (Nuclear Regulatory Commission). Design-basis tornado and tornado missiles for nuclear power plants, 1. Washington, DC: FEMA; 2007.
- [17] FBC (Florida Building Commission). Florida building code. sixth ed.; 2017. Tallahassee, FL.
- [18] ASTM International. E8/E8M-16ae1 Standard test methods for tension testing of metallic materials. 2016. West Conshohocken, PA.
- [19] FEMA P-361 Safe rooms for tornadoes and hurricanes: guidance for community and residential safe rooms. Washington, DC: Third Edit. FEMA; 2015.
- [20] B Ellingwood Development of a probability based load criterion for American National Standard A58: building code requirements for minimum design loads in buildings and other structures, 13. US Department of Commerce, National Bureau of Standards: 1980.
- [21] D Saini, B Shafei Damage assessment of wood frame shear walls subjected to lateral wind load and windborne debris impact. J Wind Eng Ind Aerod 2020;198(104091):1–13.
- [22] K Oppong, D Saini, B Shafei Vulnerability assessment of bridge piers damaged in barge collision to subsequent hurricane events. ASCE J Bridg Eng 2020. doi:10.1061/(ASCE)BE.1943-5592.0001576.
- [23] S Auyeung, A Alipour, D Saini Performance-based design of bridge piers under vehicle collision. Eng Struct 2019;191:752–765.
- [24] S AuYeung, A Alipour Evaluation of AASHTO suggested design values for reinforced concrete bridge piers under vehicle collisions. Transp Res Rec J Transp Res Board 2016;2592:1–8.
- [25] G Cowper, P Symonds Strain-hardening and strain-rate effects in the impact loading of cantilever beams. Brown Univ., Div. of Appl. Mech. No. 1957;28.
- [26] D Saini, B Shafei Investigation of concrete-filled steel tube beams strengthened with CFRP against impact loads. Compos Struct 2019;208:744–757.
- [27] D Saini, B Shafei Prediction of extent of damage to metal roof panels under hail impact. Eng Struct 2019;187:362–371.
- [28] D Saini, B Shafei Performance of concrete-filled steel tube bridge columns subjected to vehicle collision. J Bridge Eng 2019;24(8):1–13.
- [29] D Saini, B Shafei Concrete constitutive models for low velocity impact simulations. Int J Impact Eng 2019;132(103329):1–13.
- [30] T W Ipson, R F Recht Ballistic-penetration resistance and its measurement. Exp Mech 1975:15:249–257.
- [31] S Ouellet, D Cronin, M Worswick Compressive response of polymeric foams under quasi-static, medium and high strain rate conditions. Polym Test 2006:25:731–743.
- [32] L Di Landro, G Sala, D Olivieri Deformation mechanisms and energy absorption of polystyrene foams for protective helmets. Polym Test 2002;21:217–228.